Neuron
Report

Firing Rate Homeostasis in Visual Cortex of Freely Behaving Rodents

Keith B. Hengen,[1] Mary E. Lambo,[1] Stephen D. Van Hooser,[1] Donald B. Katz,[2] and Gina G. Turrigiano[1,*]
[1]Department of Biology
[2]Department of Psychology and Volen Center for Complex Systems
Brandeis University, Waltham, MA 02454, USA
*Correspondence: turrigiano@brandeis.edu
http://dx.doi.org/10.1016/j.neuron.2013.08.038

SUMMARY

It has been postulated that homeostatic mechanisms maintain stable circuit function by keeping neuronal firing within a set point range, but such firing rate homeostasis has never been demonstrated in vivo. Here we use chronic multielectrode recordings to monitor firing rates in visual cortex of freely behaving rats during chronic monocular visual deprivation (MD). Firing rates in V1 were suppressed over the first 2 day of MD but then rebounded to baseline over the next 2–3 days despite continued MD. This drop and rebound in firing was accompanied by bidirectional changes in mEPSC amplitude measured ex vivo. The rebound in firing was independent of sleep-wake state but was cell type specific, as putative FS and regular spiking neurons responded to MD with different time courses. These data establish that homeostatic mechanisms within the intact CNS act to stabilize neuronal firing rates in the face of sustained sensory perturbations.

INTRODUCTION

Experience-dependent refinement of cortical circuits is thought to require both Hebbian forms of synaptic plasticity, such as long-term potentiation (LTP) and depression (LTD), and homeostatic forms, such as synaptic scaling, that stabilize overall neuronal and circuit activity (Abbott and Nelson, 2000; Turrigiano et al., 1998). Because of the positive feedback nature of Hebbian mechanisms, they are predicted to exert a powerful destabilizing force on synaptic strengths and, if unopposed, generate network hypo- or hyperexcitability that can severely disrupt circuit function (Miller and MacKay, 1994; Turrigiano and Nelson, 2004). It has long been recognized that a simple theoretical solution to this instability problem is to endow neurons with homeostatic plasticity mechanisms that keep neuronal firing rates within a set point range (Miller and MacKay, 1994), but whether neuronal firing in the intact CNS is homeostatically regulated remains a critical and untested prediction of the neuronal homeostasis hypothesis. Here we used a monocular visual deprivation (MD) paradigm to ask whether neurons within primary visual cortex (V1) homeostatically regulate their firing rates back to a set point value during a prolonged sensory perturbation.

Visual deprivation paradigms followed by ex vivo measurements in V1 have identified several forms of Hebbian and homeostatic plasticity that are expressed in a layer- and cell-type-specific manner and are activated with distinct temporal profiles (Kirkwood et al., 1996; Rittenhouse et al., 1999; Desai et al., 2002; Maffei et al., 2006, 2010; Maffei and Turrigiano, 2008; Kaneko et al., 2008; Lambo and Turrigiano, 2013). Because of this complexity, the net effect of visual deprivation on activity within V1 is difficult to predict based on ex vivo measurements alone. Attempts to measure activity homeostasis in the intact visual cortex have not so far been definitive; in vivo calcium or intrinsic signal imaging in anesthetized animals revealed that MD first reduced and then increased visual drive (Mrsic-Flogel et al., 2007; Kaneko et al., 2008), but average visual drive was not well conserved during this process (Mrsic-Flogel et al., 2007). Visually driven activity in anesthetized animals may not be the best probe for firing rate homeostasis for a number of reasons; most critically, because homeostatic plasticity operates over a timescale of many hours (Turrigiano, 2008), it presumably normalizes some metric of average activity that will include both visually driven and spontaneous (or internally driven) spikes. We therefore set out to chronically monitor firing in V1 of freely viewing and behaving rodents over many days so that we could sample all spikes regardless of origin and directly determine whether average V1 firing rates are restored to baseline during MD.

We used a classic MD paradigm (lid suture) to perturb visual drive in juvenile rats during a developmental period (postnatal days 27–32 [P27–P32]), when this perturbation is known to induce both Hebbian and homeostatic forms of plasticity within V1 (Smith et al., 2009; Turrigiano, 2011; Levelt and Hübener, 2012). We obtained chronic multielectrode recordings as described (Jones et al., 2007; Sadacca et al., 2012; Piette et al., 2012) from both hemispheres of monocular V1 in freely behaving animals, recorded several hours of activity during the same circadian period each day for 9 days, and separated units into putative PV^+ fast-spiking basket cells (pFS) or regular-spiking units (RSUs, ~90% pyramidal). During lid suture, RSU firing rates were initially reduced (reaching a minimum on MD2) but then over the next 2–3 days rebounded to predeprivation levels. Ex vivo measurement of miniature excitatory postsynaptic currents (mEPSCs) onto L2/3 pyramidal neurons revealed a significant decrease in mEPSC amplitudes after 2 days MD,

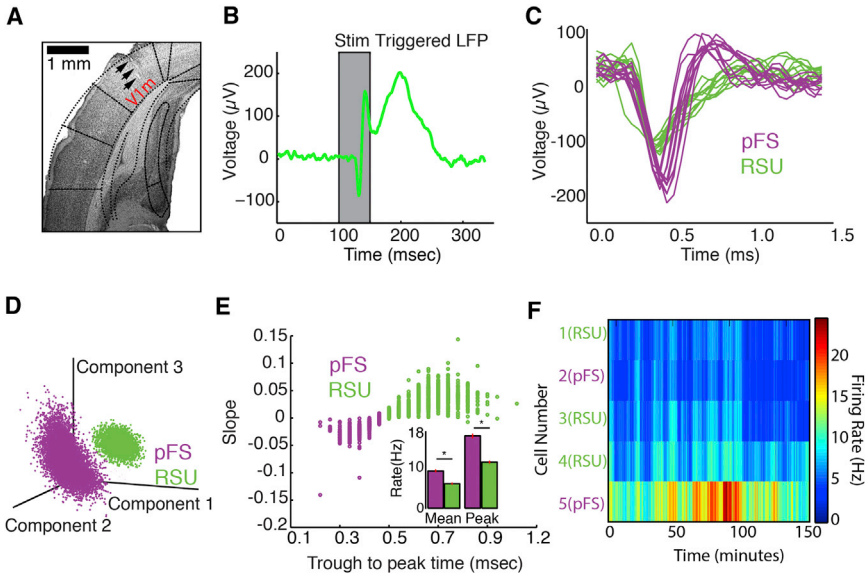

Figure 1. Chronic Multiunit Recording from V1 of Freely Behaving Rats

(A) Location of implanted microwires (arrowheads), overlaid with diagram of coronal section of rat V1m (modified from Paxinos and Watson, 1997). (B) Average LFP response from layer 2/3 to 50 × 50 ms light pulses delivered at 1 Hz (gray bar). (C) Raw traces collected on a single wire originating from two units. (D) Example of principal components clustering of units in (C). Individual spikes are represented as points in eigenspace defined by the first four principal components. The clustering algorithm identifies discrete clusters (pink and green). (E) Plot of spike trough-to-peak versus slope between 0.25 and 0.57 ms after the spike trough revealed a bimodal distribution that corresponds to pFS cells (pink) and RSUs (green). Inset: mean and peak firing rates of the RSU and pFS populations. (F) Heat map of 150 min of firing from five neurons recorded simultaneously on a single array. All error bars indicate ±SEM.

followed by an increase above baseline over the next several days. These data suggest that lid suture first suppresses RSU firing through an active LTD-like mechanism, which then activates homeostatic mechanisms (such as synaptic scaling) that restore firing precisely to baseline. This demonstrates that homeostatic mechanisms operate in the intact mammalian cortex to stabilize average firing rates in the face of sensory and plasticity-induced perturbations.

RESULTS

In order to chronically monitor firing rates in V1 of freely behaving rats, we implanted 16 channel microwire arrays bilaterally into the monocular portions of V1 (V1m) at P21. Electrode placement and depth were verified histologically at the end of each experiment (Figure 1A); activity was sampled from all layers. Full-field visual stimuli delivered in the recording chamber elicited clear stimulus-driven local field potentials (LFPs; Figure 1B). Using standard cluster-cutting techniques (Harris et al., 2000) (Figures 1C and 1D), we were able to obtain 4–16 well-isolated single units/array and could detect a similar number of units each day throughout the 9 days of recording (Figures 2C and 2D). Recordings were obtained from noon to 8 p.m. each day between P24 and P32, in an environmentally enriched recording chamber with food and water available ad libitum. MD was performed after 3 days of baseline recording (late on P26) and maintained for 6 days (through P32). A representative 150 min stretch of baseline recording is shown in Figure 1F; firing rates for individual units varied over time, and different units had distinct patterns and average levels of activity (Figures 1F and 2B).

Regular spiking pyramidal neurons comprise ~80% of neocortical neurons; to enrich for putative pyramidal neurons, we separated RSUs from pFS cells (~50% of the nonpyramidal population) using established criteria (Barthó et al., 2004; Cardin et al., 2007; Liu et al., 2009; Niell and Stryker, 2008): unlike RSUs, FS cells have a short negative-to-positive peak width and a distinct positive afterpotential that generates a negative slope 250 μs after the negative peak (Figure 1C). A plot of these two parameters for all well-isolated units revealed a bimodal distribution, with one population corresponding to pFS cell (pink) and the other corresponding to RSUs (green) (Figure 1E). The pFS population had significantly higher average and peak firing rates than RSUs, as expected (Niell and Stryker, 2008, 2010; Cardin et al., 2007; Figure 1E, inset), and RSUs in immediate proximity to pFS cells were less active immediately after a pFS spike, consistent with pFS cells being inhibitory (Figure S1 available online).

Our experimental design (Figure 2A) allowed us to manipulate visual drive to one hemisphere of V1m using monocular lid suture (MD) of the contralateral eye, while leaving visual drive to the other hemisphere unaffected; recording from both hemispheres gave us a within-animal control for any changes in activity not linked to MD. In the control hemisphere, RSU firing showed remarkable stability over the entire 9 days of recording ($n = 5$ animals, Figure 2C, ANOVA, $p = 0.98$). In marked contrast, RSU firing in the deprived hemisphere was strongly modulated by MD. Data from a representative animal are shown in Figure 2B for baseline, day 2 of MD (MD2), and MD6; while firing was depressed on MD2, firing rebounded by MD6. The same pattern was seen in the entire population of sampled units ($n = 7$ animals, Figure 2D, ANOVA, $p = 0.013$). Interestingly, on MD1, there was no reduction in firing but by MD2 average firing dropped significantly, to ~60% of baseline (Tukey-Kramer test, $p < 0.05$). This pattern is consistent with the observation that acute lid suture blurs and decorrelates visual drive but does not produce a large drop in average LGN firing rates (Linden et al., 2009) and suggests that between MD1 and MD2 decorrelated visual drive leads to an active suppression of V1m firing (Rittenhouse et al., 1999; see Discussion). Crucially, over the next 2 days of MD (MD3–MD4), firing rates rebounded and by MD5–MD6 were indistinguishable from baseline. Although mean firing rates were ~9% higher on MD6 (P32) relative to baseline (P26), this

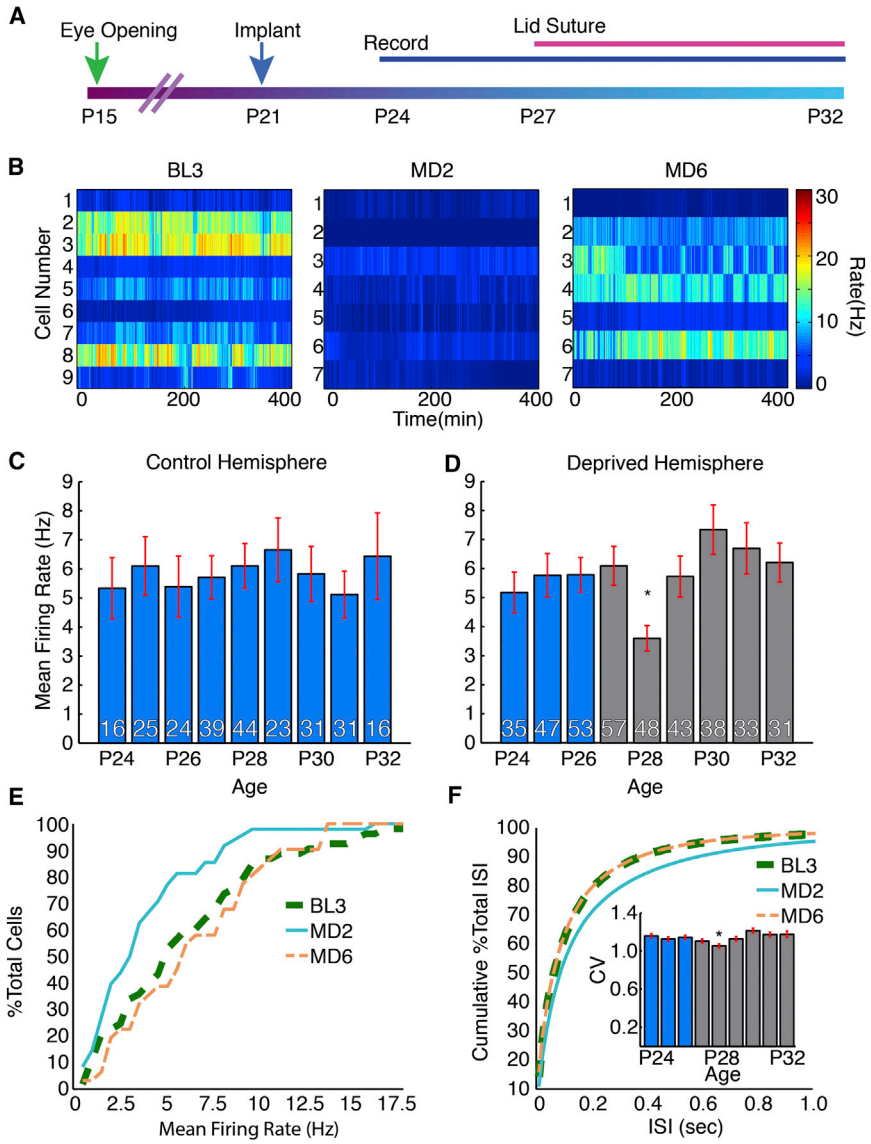

Figure 2. Homeostatic Regulation of RSU Firing during MD

(A) Experimental design. (B) Example heat maps of all recorded well-isolated RSUs from a single animal on baseline 3 (BL3), MD2, and MD6. (C and D) Average RSU firing rates in the nondeprived (control) hemisphere (C) and in the deprived hemisphere (D); here and below baseline is blue, MD is gray. Number of neurons contributing to each mean is indicated in white. (E) Distribution of mean RSU firing rates on BL3, MD2, and MD6. (F) Cumulative distribution of ISIs for BL3, MD2, and MD6; inset plots CV of ISIs, calculated for each cell and averaged. *, significantly different from BL3. All error bars indicate ±SEM.

increase was within the range of variation in the control hemisphere (Figure 2C) and was not significant ($p = 0.98$, Figure 2D, Tukey-Kramer test).

If there was a dramatic change in the number of detectable neurons before or during monocular deprivation, we might have under- or overestimated the size of the observed drop in firing and the subsequent rebound. However, the number of well-isolated units (indicated for each bar in Figure 2D) did not change significantly across days (chi-square test). Further, when we used conservative criteria to identify a subpopulation of individual RSUs we could follow for 2–6 days, this more stable population demonstrated the same biphasic pattern of firing during MD (Figures S2A–S2D). Finally, the same pattern of drop and rebound was observed when we compiled average firing by animal (Figure S2E). Thus, the drop in averaging firing rate followed by a recovery to baseline is a robust feature of individual neurons under MD.

To examine whether other aspects of neuronal firing were restored during prolonged MD, we compared the distribution of mean firing rates (Figure 2E), as well as the entire distribution of interspike intervals (ISIs) and ISI coefficient of variation (CV) (Figure 2F), as a function of days after MD. The entire distribution of mean RSU firing rates shifted to the left on MD2 (KS test, $p < 0.01$) and shifted back to become indistinguishable from baseline on MD6 (KS test, $p = 0.33$). Similarly, the entire ISI distribution shifted to the right (toward longer intervals) on MD2 (KS test, $p \leq 0.0001$) but then shifted back and by MD6 was indistinguishable from baseline (Figure 2F; KS test, $p = 0.78$). Finally, there was a small but significant reduction in CV on MD2 that also recovered.

The biphasic drop and rebound in firing that we observe here is reminiscent of the biphasic changes in mEPSC amplitude that we reported recently after MD between P22–P27 (Lambo and Turrigiano, 2013). To determine whether mEPSC amplitude undergoes a similar biphasic modulation during the MD paradigm employed here (prolonged MD between P27–P32), we sacrificed animals after 2, 4, or 6 days MD and measured mEPSC amplitude onto L2/3 pyramidal neurons in acute slices from V1m (Figure 3A). mEPSC amplitude was significantly depressed on MD2, rebounded to just above baseline by MD4, and was significantly elevated above baseline by MD6 (Figure 3A). There were no significant differences in passive neuronal properties or in mEPSC frequency between conditions. This matches well the time course of drop and rebound in RSU firing measured across all layers (Figure 2D), and when we confined our analysis to RSUs recorded from the upper layers (4–2/3), we saw a very similar pattern, with firing depressed at MD2, rebounding between MD2 and MD4, and indistinguishable from baseline by MD6 (Figure 3B). This suggests that one factor contributing to the drop and rebound in firing of RSUs during prolonged MD is the

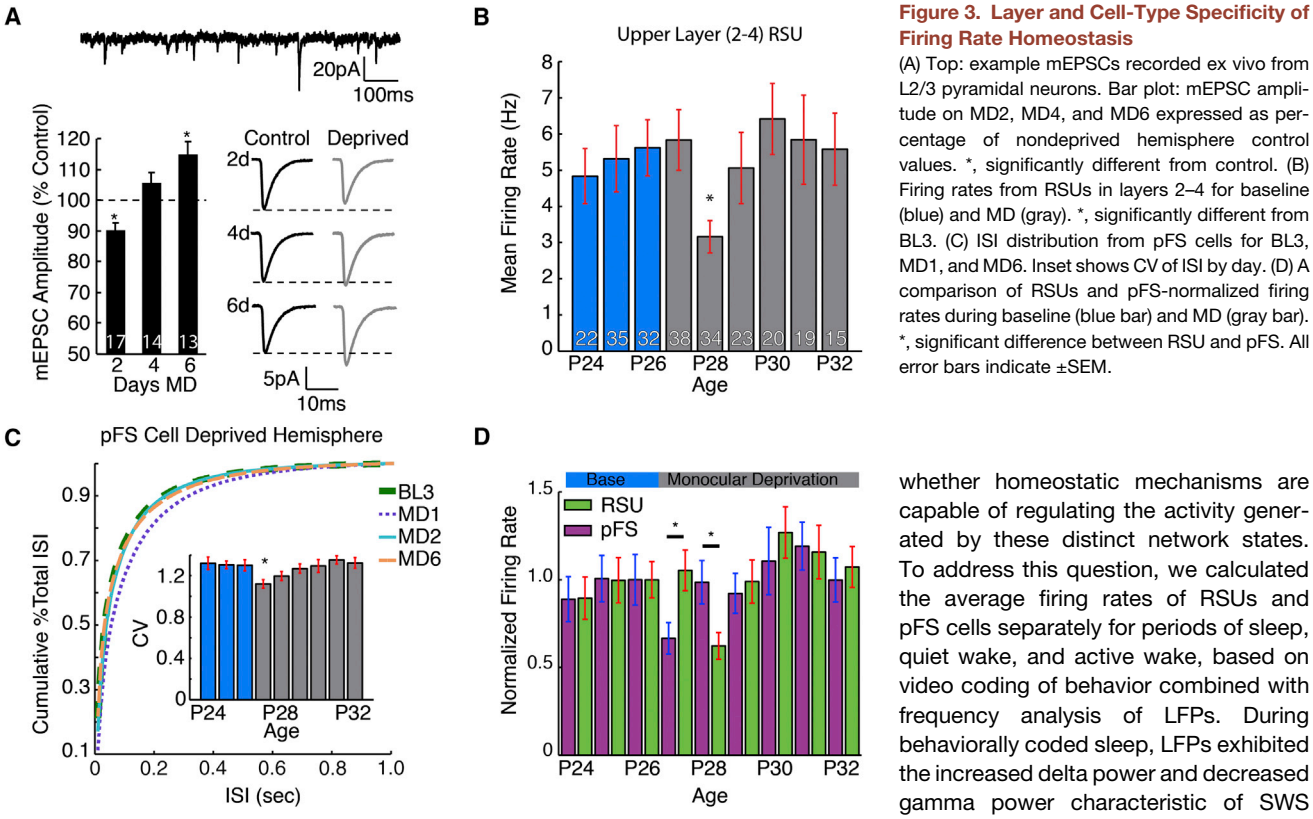

Figure 3. Layer and Cell-Type Specificity of Firing Rate Homeostasis

(A) Top: example mEPSCs recorded ex vivo from L2/3 pyramidal neurons. Bar plot: mEPSC amplitude on MD2, MD4, and MD6 expressed as percentage of nondeprived hemisphere control values. *, significantly different from control. (B) Firing rates from RSUs in layers 2–4 for baseline (blue) and MD (gray). *, significantly different from BL3. (C) ISI distribution from pFS cells for BL3, MD1, and MD6. Inset shows CV of ISI by day. (D) A comparison of RSUs and pFS-normalized firing rates during baseline (blue bar) and MD (gray bar). *, significant difference between RSU and pFS. All error bars indicate ±SEM.

bidirectional modulation of excitatory postsynaptic strength onto these neurons.

Pyramidal neurons and GABAergic interneurons serve distinct functions within the neocortical microcircuit, and it remains an open question (unaddressed even in vitro) whether firing of GABAergic interneurons is homeostatically regulated. Like RSUs, pFS firing was biphasically modulated by MD, but the timing was faster (Figures 3C and 3D), with the distribution of ISIs shifting significantly to the right (and CV decreasing; Figure 3C, inset) by MD1 ($p < 0.0005$, KS test) and returning to baseline by MD2 (KS test, $p = 0.62$) (Figure 3C). The distribution of mean firing rates was similarly modulated (Figure S3B). When pFS and RSU firing rates were normalized to allow comparison of the time course and magnitude of change, it could be seen that the pattern of drop and rebound was distinct for the two populations (Figure 3D; two-way ANOVA, $p = 0.011$); pFS firing dropped by ~33% on MD1, while RSU firing did not change until MD2 (Tukey-Kramer test), when pFS firing had largely recovered. There was no significant change in firing of pFS cells in the control hemisphere (Figure S3A; $p = 0.91$). Thus, the factors that depress and restore activity during MD are temporally distinct for these two cell types, but both undergo homeostatic recovery of firing rates.

Neocortical circuits are active across distinct behavioral states such as sleep and wake, but the patterns of activity differ (Steriade and Timofeev, 2003). Sleep and wake states are characterized by large differences in modulatory and sensory drive to cortex (Steriade, 2001; Jones, 2005), raising the question of whether homeostatic mechanisms are capable of regulating the activity generated by these distinct network states. To address this question, we calculated the average firing rates of RSUs and pFS cells separately for periods of sleep, quiet wake, and active wake, based on video coding of behavior combined with frequency analysis of LFPs. During behaviorally coded sleep, LFPs exhibited the increased delta power and decreased gamma power characteristic of SWS sleep states (Figures 4A and 4B, light green), interspersed with periods of high-frequency activity characteristic of REM (data not shown). This pattern was also apparent in single-unit activity, as a statistically significant increase in the power spectral density of spike trains in the delta power band (0.1–4 Hz) ($p < 0.01$). Quite wake included quiet sitting and grooming and could be distinguished from sleep by a drop in delta power (Figure 4A, yellow). Active wake included all active behaviors (exploration, play, motor activity, etc.) and an LFP characterized by low-delta power and high-gamma power (Figure 4B, light blue).

At the transitions between sleep and wake, the pattern of unit activity could change substantially (Figure 4C), but the ensemble firing rates averaged over these different states revealed almost identical average baseline firing rates regardless of cell type (Figures 4D and 4E). Thus, although the pattern of network activity is different across states as expected (Figures 4A–4C; Steriade, 2001), the average firing within V1 was not significantly modulated by sleep-wake transitions. In addition, when the response to MD was analyzed separately for sleep and active wake, the pattern of change was remarkably similar for the two behavioral states, for both RSUs (Figure 4D) and pFS cells (Figure 4E). Taken together, these data show that homeostatic mechanisms modulate network excitability in a manner that restores average activity across behavioral states, despite the strong differences in thalamic drive and modulatory input that characterize these states. Further, the conservation of average firing rates across states suggests that a single homeostatic target can be used to regulate neocortical stability across multiple behavioral states.

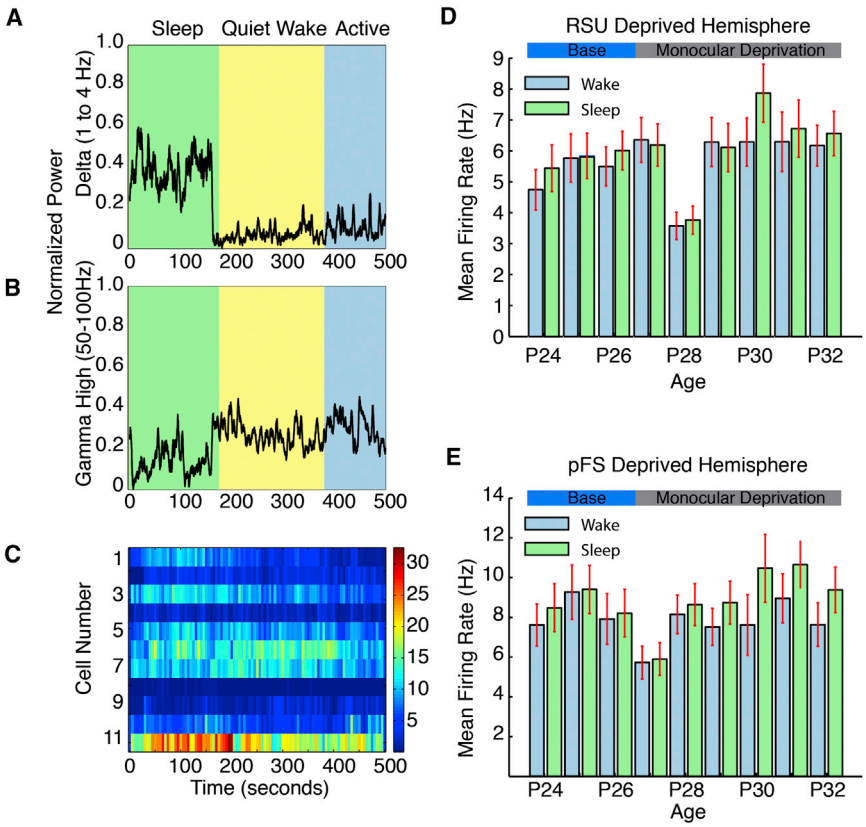

Figure 4. Firing Rate Homeostasis Is Expressed across Sleep-Wake States

(A and B) LFP delta (black trace, 1–4 Hz) (A) and gamma (B) "high" band powers during epochs of sleep (light green), quiet waking (yellow), and active wake (light blue). (C) Heat map of firing during the sleep-wake transition illustrated in (A) and (B). (D and E) RSUs (D) and pFS (E) firing rates during epochs of active wake (blue bars) and sleep (green bars) for baseline (dark blue horizontal bar) and 6 days of MD (gray horizontal bar). All error bars indicate ±SEM.

DISCUSSION

It is widely agreed that neurons require some kind of homeostatic mechanism to prevent circuit instability and runaway synaptic potentiation during experience-dependent plasticity (Abbott and Nelson, 2000; Turrigiano and Nelson, 2004; Davis 2006; Marder and Goaillard, 2006; Pozo and Goda, 2010), but the exact form this homeostatic process takes, and the aspect of neuronal activity it conserves, has not been clear. Here we show that the average firing of neocortical neurons in freely behaving animals is subject to homeostatic regulation. We used chronic multielectrode recordings from V1 to follow ensemble firing rates over time before and during prolonged MD and found that while firing decreased over the first 2 days of MD, over the next 2–3 days firing was restored to baseline despite continued MD. The time course of this drop and recovery was cell type specific, was correlated with changes in mEPSC amplitude, and was manifested across sleep-wake states. These data establish that homeostatic mechanisms within the intact CNS act to stabilize neuronal firing rates in the face of sensory perturbations.

Because we followed ensemble average firing rates, we do not know for certain that the average firing rates of individual neurons are restored to their predeprivation values. It is suggestive that the distribution of average firing rates for baseline and MD6 is indistinguishable (Figure 2E), consistent with the interpretation that homeostatic regulation of firing in vivo is a cell-autonomous process that restores individual neurons back to an individual set point. However, we cannot exclude the alternative possibility that it is the ensemble average that is regulated, while firing rates of individual neurons change over time and come to occupy a different point in the distribution. This would necessitate some kind of competitive network-level mechanism that enhances average firing of some neurons at the expense of others to maintain the ensemble average (Hirase et al., 2001). While no such circuit-level mechanism has been identified within neocortex, there is strong evidence that neocortical neurons express cell-autonomous forms of homeostatic plasticity that could serve to regulate average firing (Desai et al., 2002; Maffei and Turrigiano, 2008; Lambo and Turrigiano, 2013). Thus, the most likely scenario is that firing rate homeostasis is implemented in a cell-autonomous manner and that there is a broad distribution of firing rate set points across neocortical neurons. Interestingly, heterogeneity in the homeostatic set point has been shown to improve performance in a network model of working memory (Renart et al., 2003), suggesting that this heterogeneity could be of biological significance.

Acute lid suture abolishes stimulus-driven activity but has little effect on spontaneous thalamic firing rates (Linden et al., 2009), which may in part explain why there is no immediate drop in RSU firing on MD1. A second important factor is the drop in firing of pFS cells at MD1, which may temporarily boost RSU activity by reducing inhibition from FS cells. Over time the desynchronized pre- and postsynaptic firing induced by lid suture is predicted to induce LTD (Linden et al., 2009), and the drop in RSU firing on MD2 correlates well with the induction of LTD within V1. Two days of MD during the critical period (P21–P33) induces depression of thalamocortical and intracortical excitatory synapses (Heynen et al., 2003; Khibnik et al., 2010; Maffei and Turrigiano, 2008; Wang et al., 2013) and occludes the ex vivo induction of LTD (Heynen et al., 2003), and we show here that the reduction in RSU firing after 2 days MD is correlated with a reduction in the amplitude of mEPSCs onto L2/3 pyramidal neurons. This suggests that the time course of the drop in firing we observe for RSUs following MD, with no change at MD1 and a significant drop by MD2, is driven in part by the induction of

LTD at thalamocortical and intracortical synapses, including synapses within L2/3. A second factor is likely to be the rebound in pFS firing rates by MD2, which should recruit additional inhibition onto RSUs. While FS cells are known to undergo ocular dominance shifts (Aton et al., 2013; Yazaki-Sugiyama et al., 2009), little is known about the forms or timing of plasticity at synapses onto FS cells during MD. It is thus unclear why the drop and rebound in firing for pFS and RSUs have distinct temporal profiles.

While the early phase of MD is correlated with the induction of LTD, we show that the slow restoration of firing to baseline between MD2 and MD4–MD5 is correlated with a homeostatic increase in mEPSC amplitude onto L2/3 pyramidal neurons. Interestingly, mEPSC amplitude does not simply return to baseline but trends toward potentiation by MD4 and becomes significantly potentiated by MD6, indicating that this potentiation is not a simple reversal of LTD. This potentiation is likely due to homeostatic synaptic scaling rather than an LTP-like mechanism, as it relies critically on GluA2 C-tail interactions (a signature of synaptic scaling, Gainey et al., 2009; Lambo and Turrigiano, 2013) and occurs despite the lack of correlated visual drive thought to be necessary for LTP induction (Smith et al., 2009). The temporal and mechanistic dissociation between a depressive and a homeostatic phase of MD-induced plasticity is also suggested by the observation that TNFα signaling (which is necessary for the expression of synaptic scaling) is dispensable for the early decrease in visual responsiveness but is necessary for the slower rebound in responsiveness between MD2 and MD6 (Kaneko et al., 2008). Taken together, these data suggest that synaptic scaling up of intracortical synapses is one mechanism that contributes to the homeostatic restoration of RSU firing rates. Because neocortical microcircuits are complex and recurrent, and many forms of plasticity exist at many sites within these circuits (Nelson and Turrigiano, 2008), it is highly likely that other forms of plasticity in addition to LTD and synaptic scaling contribute to the sequential depression and homeostatic rebound in RSU firing rates that we observe here. What our data establish is that the net effect of all of these plastic mechanisms is the precise restoration of firing rates in the face of continued sensory deprivation.

An interesting finding of this study is that both pFS and RSUs undergo firing rate homeostasis. This suggests that conservation of firing rates is functionally important for both cell types, perhaps because it maintains an excitability regime in which each cell type is able to respond effectively to its inputs. The rebound in pFS firing rates on MD2 means that to restore RSU firing rates, homeostatic mechanisms must adjust excitation enough to precisely compensate both for the induction of LTD and for the rebound in pFS firing rates (which should recruit more inhibition onto RSUs). Because other (non-FS) classes of GABAergic interneurons cannot be cleanly differentiated from pyramidal neurons in these extracellular recordings, it is not clear whether all GABAergic neuron types express firing rate homeostasis, or if this is a property confined to pyramidal and FS cells.

One puzzling question raised by the firing rate homeostasis hypothesis is how a homeostatic activity target can be implemented in a network that operates under very different sensory and modulatory conditions during different behavioral states (Steriade and Timofeev, 2003; Vyazovskiy et al., 2009). Because rodents sleep in short bouts interspersed with periods of active wake, our data provide a well-controlled opportunity to explore this question. One possibility is that neocortical networks have different set points during fundamentally different behavioral states. Another possibility is that homeostatic regulation only constrains the activity of neurons in certain states (wake, for example), while firing rates during other states (such as sleep) are largely unregulated. Surprisingly, our data point to a third possibility: homeostatic mechanisms are implemented in neocortical circuits so as to maintain a single firing rate set point across sleep-wake states. Although we found differences in the pattern of firing across ensembles of neurons at the transitions between sleep and wake, firing rates averaged over many bouts of sleep or interspersed active wake were not significantly different. These results are consistent with one report in hippocampus (Hirase et al., 2001), while another report found small differences in average neocortical firing rates between end of wake and end of sleep (Vyazovskiy et al., 2009), and a third found larger differences in neocortical firing ($\sim$50%) when comparing maze running to subsequent sleep in a sleep box (Vijayan et al., 2010). Notably, the later two studies averaged activity over much shorter periods of time and did not control for possible circadian or environmental effects on firing. Our data show that when these factors are controlled, average V1 firing rates are conserved across sleep-wake states and suggest that a single homeostatic set point can be used to regulate activity in both states. Further, both states exhibited the same magnitude and timing of homeostatic restoration of average firing. This demonstrates that the mechanisms that restore firing in V1 can constrain the average firing of networks as they switch rapidly between very different conditions of sensory and modulatory drive.

EXPERIMENTAL PROCEDURES

All surgical techniques and experimental procedures were conducted in accordance with the Brandeis University IACUC and NIH guidelines.

In Vivo Data Collection and Analysis

Seven juvenile Long-Evans rats of both sexes (P21) were implanted bilaterally with custom 16-channel 33 μm tungsten microelectrode arrays (Tucker-Davis Technologies) into V1; location was confirmed post hoc via histological reconstruction. After 2 days of recovery, data were collected for 3 days of baseline (P24–P26) and 6 days of monocular lid suture (Lambo and Turrigiano, 2013) (P27–P32). Recordings were conducted daily between noon (zeitgeber time [ZT] 04:30) and 8:00 p.m. (ZT 12:30), in an environmentally enriched recording chamber (12" × 12") with food and water available ad libitum and two littermates for social stimulation.

Neuronal signals were amplified, digitized, sampled at 25 kHz by commercially available hardware (Tucker-Davis), and saved for offline analyses using custom software (MATLAB). Briefly, data were high-pass filtered (500 Hz) and spike waveforms were extracted based on a voltage threshold and sorted offline into single units with a semiautomatic clustering algorithm (Harris et al., 2000) in four dimensions formed by principal components. Cluster isolation and quality was evaluated by thresholding of L-Ratio and Mahalanobis distance (Schmitzer-Torbert et al., 2005), as well as the MSE of unit averages over time. Clusters from two or more units that could not be cleanly divided were classified as multiunit traces and excluded from single-unit analyses. Researchers were blind to experimental condition during clustering. The data are reported as mean ± SEM unless otherwise noted. A one-way ANOVA followed

by post hoc Tukey-Kramer tests was used to determine statistical significance ($p < 0.05$) unless otherwise noted.

Behavioral Analyses

Animals in the recording chamber were continuously video monitored and scored for behavioral state offline. Behavior was divided into three categories: "Active Wake," which included any locomotor activity; "Quiet Wake," which included grooming and quiescent periods with small movements and obvious postural stability; and "Sleep," which included long periods of motionless quiescence and lack of postural tone. Behavioral scoring was compared to the LFP delta band power (1–4 Hz, Chebyshev Type II filter, MATLAB) to confirm the accuracy of sleep scoring in a subset of animals (n = 3). All behaviorally scored epochs of sleep demonstrated increases in delta band power.

Slice Preparation and mEPSC Recordings

After MD on P26, coronal brain slices (300 μm) containing V1m were prepared on P28, P30, and P32; recording conditions and analysis were as previously described (Lambo and Turrigiano, 2013, details in Supplemental Experimental Procedures).

SUPPLEMENTAL INFORMATION

Supplemental Information includes Supplemental Experimental Procedures and three figures and can be found with this article online at http://dx.doi.org/10.1016/j.neuron.2013.08.038.

ACKNOWLEDGMENTS

We thank Brian Sadacca and Caitlin Piette for help with surgeries and James McGregor for help with behavioral coding. This work was supported by NIH grant NS036853 (G.G.T.), NSF CELEST 4500000382 (hosted by BU), and NRSA F32 NS078859 (K.B.H.).

Accepted: August 29, 2013
Published: October 16, 2013

REFERENCES

Abbott, L.F., and Nelson, S.B. (2000). Synaptic plasticity: taming the beast. Nat. Neurosci. *3*(*Suppl*), 1178–1183.

Aton, S.J., Broussard, C., Dumoulin, M., Seibt, J., Watson, A., Coleman, T., and Frank, M.G. (2013). Visual experience and subsequent sleep induce sequential plastic changes in putative inhibitory and excitatory cortical neurons. Proc. Natl. Acad. Sci. USA *110*, 3101–3106.

Barthó, P., Hirase, H., Monconduit, L., Zugaro, M., Harris, K.D., and Buzsáki, G. (2004). Characterization of neocortical principal cells and interneurons by network interactions and extracellular features. J. Neurophysiol. *92*, 600–608.

Cardin, J.A., Palmer, L.A., and Contreras, D. (2007). Stimulus feature selectivity in excitatory and inhibitory neurons in primary visual cortex. J. Neurosci. *27*, 10333–10344.

Davis, G.W. (2006). Homeostatic control of neural activity: from phenomenology to molecular design. Annu. Rev. Neurosci. *29*, 307–323.

Desai, N.S., Cudmore, R.H., Nelson, S.B., and Turrigiano, G.G. (2002). Critical periods for experience-dependent synaptic scaling in visual cortex. Nat. Neurosci. *5*, 783–789.

Gainey, M., Hurvitz-Wolff, J., Lambo, M., and Turrigiano, G.G. (2009). Synaptic scaling requires the GluR2 subunit of the AMPA receptor. J. Neurosci. *29*, 6479–6489.

Harris, K.D., Henze, D.A., Csicsvari, J., Hirase, H., and Buzsáki, G. (2000). Accuracy of tetrode spike separation as determined by simultaneous intracellular and extracellular measurements. J. Neurophysiol. *84*, 401–414.

Heynen, A.J., Yoon, B.J., Liu, C.H., Chung, H.J., Huganir, R.L., and Bear, M.F. (2003). Molecular mechanism for loss of visual cortical responsiveness following brief monocular deprivation. Nat. Neurosci. *6*, 854–862.

Hirase, H., Leinekugel, X., Czurkó, A., Csicsvari, J., and Buzsáki, G. (2001). Firing rates of hippocampal neurons are preserved during subsequent sleep episodes and modified by novel awake experience. Proc. Natl. Acad. Sci. USA *98*, 9386–9390.

Jones, B.E. (2005). From waking to sleeping: neuronal and chemical substrates. Trends Pharmacol. Sci. *26*, 578–586.

Jones, L.M., Fontanini, A., Sadacca, B.F., Miller, P., and Katz, D.B. (2007). Natural stimuli evoke dynamic sequences of states in sensory cortical ensembles. Proc. Natl. Acad. Sci. USA *104*, 18772–18777.

Kaneko, M., Stellwagen, D., Malenka, R.C., and Stryker, M.P. (2008). Tumor necrosis factor-alpha mediates one component of competitive, experience-dependent plasticity in developing visual cortex. Neuron *58*, 673–680.

Khibnik, L.A., Cho, K.K., and Bear, M.F. (2010). Relative contribution of feedforward excitatory connections to expression of ocular dominance plasticity in layer 4 of visual cortex. Neuron *66*, 493–500.

Kirkwood, A., Rioult, M.C., and Bear, M.F. (1996). Experience-dependent modification of synaptic plasticity in visual cortex. Nature *381*, 526–528.

Lambo, M.E., and Turrigiano, G.G. (2013). Synaptic and intrinsic homeostatic mechanisms cooperate to increase L2/3 pyramidal neuron excitability during a late phase of critical period plasticity. J. Neurosci. *33*, 8810–8819.

Levelt, C.N., and Hübener, M. (2012). Critical-period plasticity in the visual cortex. Annu. Rev. Neurosci. *35*, 309–330.

Linden, M.L., Heynen, A.J., Haslinger, R.H., and Bear, M.F. (2009). Thalamic activity that drives visual cortical plasticity. Nat. Neurosci. *12*, 390–392.

Liu, B.H., Li, P., Li, Y.T., Sun, Y.J., Yanagawa, Y., Obata, K., Zhang, L.I., and Tao, H.W. (2009). Visual receptive field structure of cortical inhibitory neurons revealed by two-photon imaging guided recording. J. Neurosci. *29*, 10520–10532.

Maffei, A., and Turrigiano, G.G. (2008). Multiple modes of network homeostasis in visual cortical layer 2/3. J. Neurosci. *28*, 4377–4384.

Maffei, A., Nataraj, K., Nelson, S.B., and Turrigiano, G.G. (2006). Potentiation of cortical inhibition by visual deprivation. Nature *443*, 81–84.

Maffei, A., Lambo, M.E., and Turrigiano, G.G. (2010). Critical period for inhibitory plasticity in rodent binocular V1. J. Neurosci. *30*, 3304–3309.

Marder, E., and Goaillard, J.M. (2006). Variability, compensation and homeostasis in neuron and network function. Nat. Rev. Neurosci. *7*, 563–574.

Miller, K.D., and MacKay, D.J.C. (1994). The role of constraints in Hebbian learning. Neural Comput. *6*, 100–126.

Mrsic-Flogel, T.D., Hofer, S.B., Ohki, K., Reid, R.C., Bonhoeffer, T., and Hübener, M. (2007). Homeostatic regulation of eye-specific responses in visual cortex during ocular dominance plasticity. Neuron *54*, 961–972.

Nelson, S.B., and Turrigiano, G.G. (2008). Strength through diversity. Neuron *60*, 477–482.

Niell, C.M., and Stryker, M.P. (2008). Highly selective receptive fields in mouse visual cortex. J. Neurosci. *28*, 7520–7536.

Niell, C.M., and Stryker, M.P. (2010). Modulation of visual responses by behavioral state in mouse visual cortex. Neuron *65*, 472–479.

Paxinos, G., and Watson, C. (1997). The Rat Brain in Stereotaxic Coordinates. (San Diego: Academic Press).

Piette, C.E., Baez-Santiago, M.A., Reid, E.E., Katz, D.B., and Moran, A. (2012). Inactivation of basolateral amygdala specifically eliminates palatability-related information in cortical sensory responses. J. Neurosci. *32*, 9981–9991.

Pozo, K., and Goda, Y. (2010). Unraveling mechanisms of homeostatic synaptic plasticity. Neuron *66*, 337–351.

Renart, A., Song, P., and Wang, X.J. (2003). Robust spatial working memory through homeostatic synaptic scaling in heterogeneous cortical networks. Neuron *38*, 473–485.

Rittenhouse, C.D., Shouval, H.Z., Paradiso, M.A., and Bear, M.F. (1999). Monocular deprivation induces homosynaptic long-term depression in visual cortex. Nature *397*, 347–350.

Sadacca, B.F., Rothwax, J.T., and Katz, D.B. (2012). Sodium concentration coding gives way to evaluative coding in cortex and amygdala. J. Neurosci. *32*, 9999–10011.

Schmitzer-Torbert, N., Jackson, J., Henze, D., Harris, K., and Redish, A.D. (2005). Quantitative measures of cluster quality for use in extracellular recordings. Neuroscience *131*, 1–11.

Smith, G.B., Heynen, A.J., and Bear, M.F. (2009). Bidirectional synaptic mechanisms of ocular dominance plasticity in visual cortex. Philos. Trans. R. Soc. Lond. B Biol. Sci. *364*, 357–367.

Steriade, M. (2001). Impact of network activities on neuronal properties in corticothalamic systems. J. Neurophysiol. *86*, 1–39.

Steriade, M., and Timofeev, I. (2003). Neuronal plasticity in thalamocortical networks during sleep and waking oscillations. Neuron *37*, 563–576.

Turrigiano, G.G. (2008). The self-tuning neuron: synaptic scaling of excitatory synapses. Cell *135*, 422–435.

Turrigiano, G.G. (2011). Too many cooks? Intrinsic and synaptic homeostatic mechanisms in cortical circuit refinement. Annu. Rev. Neurosci. *34*, 89–103.

Turrigiano, G.G., and Nelson, S.B. (2004). Homeostatic plasticity in the developing nervous system. Nat. Rev. Neurosci. *5*, 97–107.

Turrigiano, G.G., Leslie, K.R., Desai, N.S., Rutherford, L.C., and Nelson, S.B. (1998). Activity-dependent scaling of quantal amplitude in neocortical neurons. Nature *391*, 892–896.

Vijayan, S., Hale, G.J., Moore, C.I., Brown, E.N., and Wilson, M. (2010). Activity in the barrel cortex during active behavior and sleep. J. Neurophysiol. *103*, 2074–2084.

Vyazovskiy, V.V., Olcese, U., Lazimy, Y.M., Faraguna, U., Esser, S.K., Williams, J.C., Cirelli, C., and Tononi, G. (2009). Cortical firing and sleep homeostasis. Neuron *63*, 865–878.

Wang, L., Kloc, M., Gu, Y., Ge, S., and Maffei, A. (2013). Layer-specific experience-dependent rewiring of thalamocortical circuits. J. Neurosci. *33*, 4181–4191.

Yazaki-Sugiyama, Y., Kang, S., Câteau, H., Fukai, T., and Hensch, T.K. (2009). Bidirectional plasticity in fast-spiking GABA circuits by visual experience. Nature *462*, 218–221.